Low-cost, high performance surface plasmon resonance-compatible films characterized by the surface plasmon resonance technique*

Li Song-Quan(李松权), Ye Hong-An(叶红安)†, Liu Chun-Yu(柳春郁), Dou Yin-Feng(窦寅丰), and Huang Yan(黄 妍)

School of Electronic Engineering, Heilongjiang University, Harbin 150080, *China*

(Received 25 December 2012; revised manuscript received 18 January 2013)

A new analytical method based on the surface plasmon resonance (SPR) technique is presented, with which SPR curves for both wavelength and angular modulations can be obtained simultaneously via only a single scan of the incident angle. Using this method, the SPR responses of TiO_2-coated Cu films are characterized in the wavelength range from 600 nm to 900 nm. For the first time, we determine the effective optical constants and the thicknesses of TiO_2-coated Cu films using the SPR curves of wavelength modulation. The sensitivities of prism-based SPR refractive index sensors using TiO_2-coated Cu films are investigated theoretically for both wavelength and angular modulations, the results show that in the case of sensitivity with wavelength modulation, TiO_2-coated Cu films are not as good as the Au film, however, they are more suitable than the Au film for SPR refractive index sensors with angular modulation because a higher sensitivity can be achieved.

Keywords: surface plasmon resonance, optical constants, thin film

PACS: 73.20.Mf, 78.20.–e **DOI:** 10.1088/1674-1056/22/7/077302

1. Introduction

Noble metals such as Au and Ag are the most widely used metals in surface plasmon resonance (SPR) experiments due to their advantages: they display SPR bands in both the visible and the near-infrared (NIR) frequencies, their surface chemistry is well-characterized, and they are easily functionalized for biosensing. However, Au and Ag also suffer from some disadvantages: they are expansive, especially the Au films; silver films tarnish rapidly in ambient conditions. Because of these problems, several SPR-compatible films[1–9] that are chemically and mechanically robust have been produced. Among the SPR-compatible metals, Al has received much attention and many investigations gave important information on the SPR phenomenon of Al films.[10–18] Recently, Al/TiO_2 film has been used in SPR optical fiber sensors owing to its response in the NIR region, especially in the 1500 nm region.[19] Cu film has also been used as an SPR sensor element,[16] however, no sufficient investigations on the SPR sensing properties of the Cu film have been carried out due to its unstable chemical properties as compared to Au, Ag, and Al films.

Many previous studies on the optical properties of Cu have been reported, the optical constants of Cu covering a wide frequency domain and their dependences of temperature, crystallographic orientation, surface roughness, and oxidation have been investigated.[20–32] It was confirmed that the optical constants of Cu are related to a threshold for the interband electronic transitions accounting for the sudden change in the imaginary part of optical constants $\varepsilon_i(\lambda)$ between 550 nm and 600 nm, while in the wavelength range from 650 nm to 2500 nm, the dielectric constants can be determined almost entirely by free electrons without considering the contribution of any bound electrons.[21] Therefore, the optical properties of the Cu film, especially in the red and infrared wavelength range, should be paid more attention to when the Cu film is used as an active layer for SPR.

Cu is prone to surface oxidation upon exposure to ambient laboratory atmosphere at room temperature, in this case, the dominant product is Cu_2O and the minor product is CuO.[16,32] Various protection methods have been implemented to prevent the oxidation of Cu, for example, embedding Cu nanoparticles into a transparent matrix to prevent the oxidation and to study their optical properties, fabricating nanoparticles in a solution; removing oxides by using glacial acetic acid or heating the Cu sample in vacuum to a high temperature.[32] The protection of Cu from corrosion is also necessary for stable use when the Cu film is utilized in an SPR experiment. Commonly, an overlayer deposited on a metal film is employed to protect the oxidable surface, tune the measureable range of the sensor by affecting the resonance condition, or improve the performance of the sensor. One alternative is to use metal. Bimetallic layers comprised of Ag and Au are used as SPR-compatible layers, in which the Au film is also an overlayer.[33–36] It is well known that they combine the advantages of both Ag and Au layers, however, the combination shows significant aging effects which degrade the intrinsic sensitivity of the sensor chips.[36] Another alternative is to use layers of other materials. The

*Project supported by the National Natural Science Foundation of China (Grant No. 61177079) and the Young Scientists Fund of the National Natural Science Foundation of China (Grant No. 61205071).

†Corresponding author. E-mail: yehonganhlj@gmail.com

© 2013 Chinese Physical Society and IOP Publishing Ltd

films of metal and semiconductor oxides are widely used as overlayers,[37] and they might be more suitable for overlayers due to their low cost as well as maximum allowable thicknesses related to their refractive indexes in the design process of SPR devices. Among oxides, TiO_2 has been extensively studied in the form of thin films for optical applications and received much attention in sensing applications due to good sensing properties towards humidity, oxygen, and organic vapors, as well as hazardous or toxic gases.[38–44]

The SPR technique is an accurate and simple method for the determination of optical constants and thicknesses of SPR-compatible films.[45–49] In calculation process, the one-layer model is generally used, the metal film is considered to be homogeneous, and the interfaces are perfectly flat in the model, the surface roughness is not considered. To describe the influence of the surface roughness and deduce more reasonable results, a multilayer model consisting of an intermediate layer is used, and the intermediate layer is modeled by using the effective medium approximation.[50] Nevertheless, the one-layer model is more convenient and also good enough to characterize the SPR-compatible films by providing the effective properties which are also related to the internal structure.

In SPR sensors, a surface plasmon wave (SPW) is excited at the interface between SPR-compatible film and dielectric medium. The changes in the refractive index of the dielectric medium are then measured. A change in the refractive index of the dielectric medium produces a change in the propagation constant of the SPW. Based on which characteristic of the light wave interacting with the SPW is measured, SPR sensors can be classified into SPR sensors with angular or wavelength modulation, and so on.[51] In SPR experiments with angular modulation, the SPR curve $R(\theta)$ can be generated through scanning the angle of incidence step by step at a given wavelength. In the case of wavelength modulation, the SPR curve $R(\lambda)$ can be obtained by using a light beam from a broadband source when the angle of incidence is appropriately fixed.

This work aims to study the TiO_2-coated Cu film via the SPR response of the film and the sensitivity of the SPR refractive index sensor in which the film is employed. For this purpose, SPR curves of wavelength and angular modulations are obtained simultaneously via only a single scan of the incident angle. This method is particularly suit for studying the SPR response of a film due to its distinct advantage of convenience. Using this method, the SPR responses of an Au film and the TiO_2-coated Cu films are characterized in a wavelength range from 600 nm to 900 nm at room temperature. Using the algorithm reported previously by us,[52] we determine the effective optical constants and thicknesses of the films by using SPR curves $R(\lambda)$. To our knowledge, it is the first time that the effective optical properties of TiO_2-coated Cu films have been determined by using the SPR technique. To study the sensitivities of the prism-based SPR refractive index sensors in which the TiO_2-coated Cu films are employed, the sensitivities are investigated theoretically and compared to that of the Au film both for wavelength and angular modulations. The results show that even though for sensitivity with wavelength modulation, the TiO_2-coated Cu films are not as good as the Au film, a higher sensitivity can be achieved for sensors with angular modulation in which the TiO_2-coated Cu films are employed.

2. Experimental details

BK7 glass substrates were sourced from Agar Scientific Ltd, and were cleaned with acetone, ethanol then soaked in a detergent solution before de-ionized water rinse and nitrogen dry. Cu and TiO_2 films could be applied either by sputtering or e-beam deposition, we chose the e-beam deposition because it is the most consistent method. The Au film (56 nm) was prepared by evaporating 99.999% pure gold onto the substrates. The Cu film was deposited on the substrates followed by TiO_2 in a vacuum chamber. Three TiO_2-coated Cu films were prepared, which had a Cu film of the same thickness (56 nm) and a TiO_2 film of different thickness (5 nm, 10 nm, 14.6 nm). The evaporation rates and the thicknesses were monitored by an IC/5 thin film deposition controller (INFICON) with a 6 MHz Au-coated crystal. For the purpose of the present work, four samples have been prepared, and the corresponding films are denoted as Au0, Cu1, Cu2, and Cu3.

A measurement apparatus was built up to investigate the plasmoinc properties of the SPR-compatible films, as shown in Fig. 1. A well collimated light beam from a broadband source (Tungsten halogen light source, AvaLight-Hal) is p-polarized by a Glan–Taylor polarizer to excite the SPWs. The p-polarized light is coupled to the surface plasmon via Kretschmann's prism configuration. The reflected light from the SPR-compatible films is monitored by an optic spectrometer (Ocean Optics USB4000), from which we can obtain the SPR curve $R(\lambda)$. As depicted in Fig. 1, an adaptive optical structure is used,[53] in which a rhombohedral BK7 prism consists of two prisms (isosceles right-angled triangle) affixed each other with index-matching fluid. The fluid is also used to attach a sample to a face of the hypotenuse side of the triangle prism. The rhombohedral prism is mounted on a computer-controlled rotary stage to scan the angle of incidence, and the parallel shift of the incident light beam is implemented simultaneously utilizing a computer-controlled translation stage. With this configuration, the light beam is able to incident upon almost the same region of a film, and the light output from the prism is always parallel to the incident light during the scanning, which brings great convenience for detection. The total internal reflection (TIR) spectrum of the light from the broadband source reflected from the part of prism without attached substrate is measured and taken as the reference spectrum for calibration.

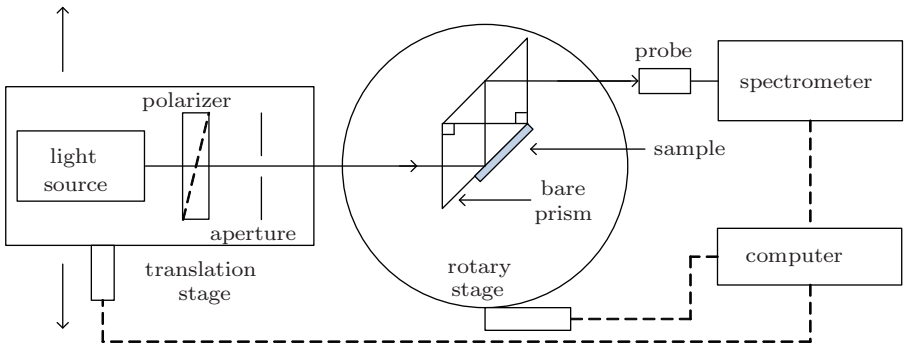


Fig. 1. Schematic diagram of the measurement apparatus.

3. Results and analyses

A series of SPR curves $R(\lambda)$ are generated through scanning the angle of incidence. The SPR curves $R(\theta)$ for each film at corresponding resonant wavelengths are extracted from the normalized SPR curves $R(\lambda)$. In the extracting process, the values of incidence angles against the films at each resonant wavelength are corrected considering the dispersion effect of the prism.

The normalized SPR curves $R(\lambda)$ for the films are shown in Figs. 2–5. High-quality SPR curves $R(\lambda)$ are prohibited in the long-wavelength region due to the degraded signal-to-noise ratio associated with the response of the spectrometer and the SPR responses of the films.

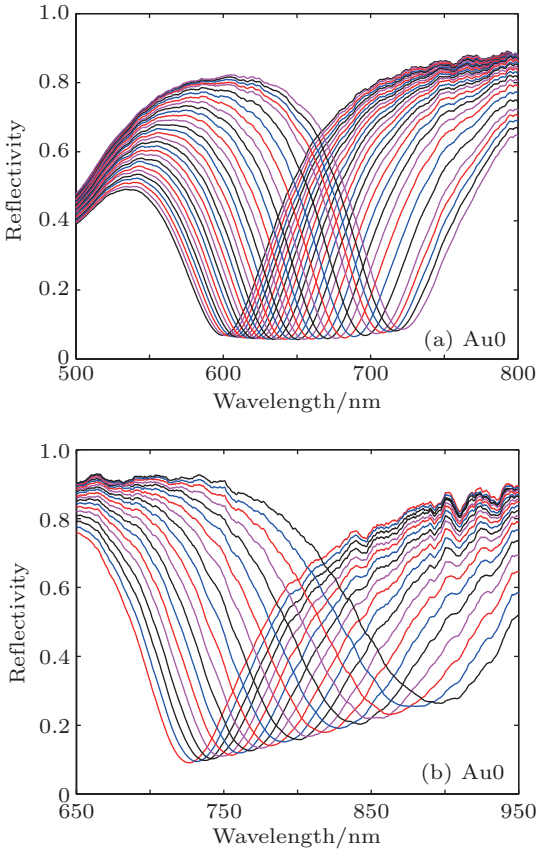


Fig. 2. (color online) Normalized SPR curves $R(\lambda)$ of Au0 in the wavelength ranges: (a) from 600.04 nm to 726.69 nm, (b) from 734.90 nm to 896.06 nm.

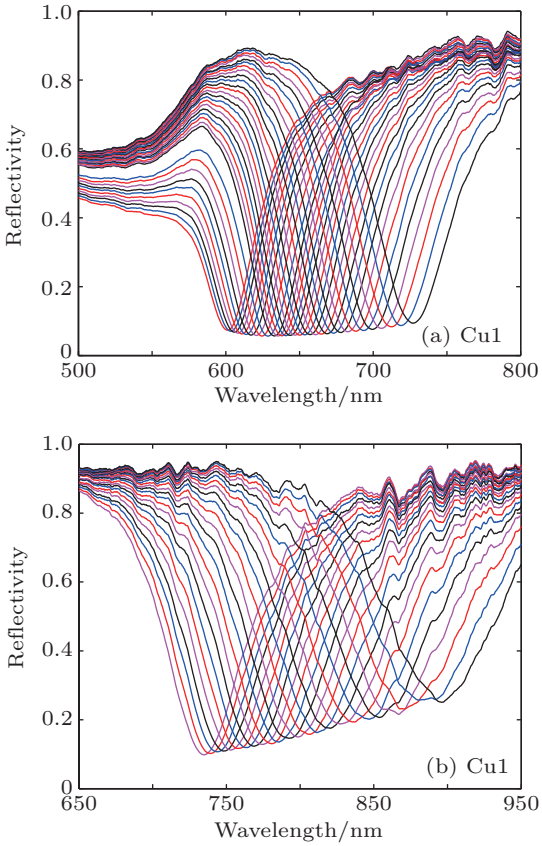


Fig. 3. (color online) Normalized SPR curves $R(\lambda)$ of Cu1 in the wavelength ranges: (a) from 601.45 nm to 726.69 nm, (b) from 734.90 nm to 896.06 nm.

The SPR curves $R(\theta)$ for each film at corresponding resonant wavelengths are extracted from the normalized SPR curves $R(\lambda)$. In the extracting process, the values of incidence angles against the films at each resonant wavelength are corrected considering the dispersion effect of the prism. In addition, to get the width information of SPR curves $R(\theta)$, we can only investigate SPR curves $R(\theta)$ at the wavelengths in the middle of the wavelength region we studied. However, we can also obtain SPR curves $R(\theta)$ at other wavelengths which are not the resonant wavelengths in the middle range. The disadvantage is that the information of resonant angle and corresponding minimum reflectivity cannot be obtained directly.

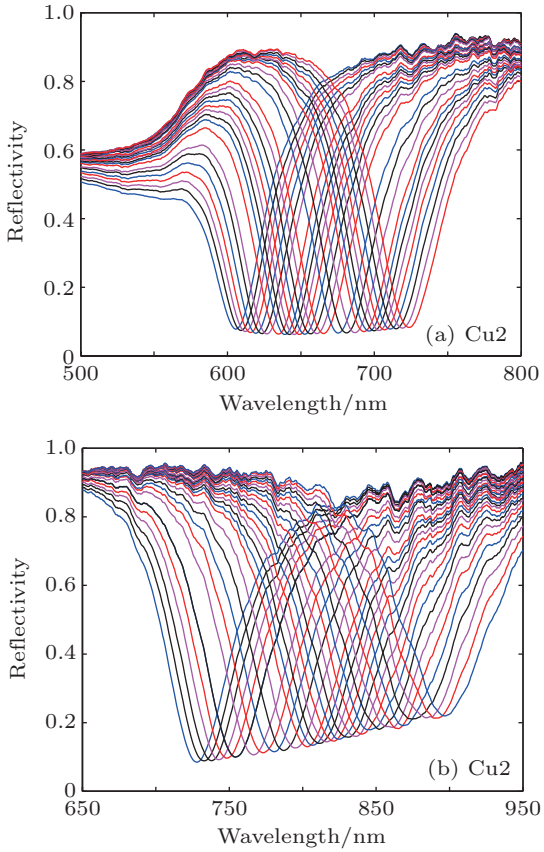


Fig. 4. (color online) Normalized SPR curves $R(\lambda)$ of Cu2 in the wavelength ranges: (a) from 605.67 nm to 723.63 nm, (b) from 728.03 nm to 896.94 nm.

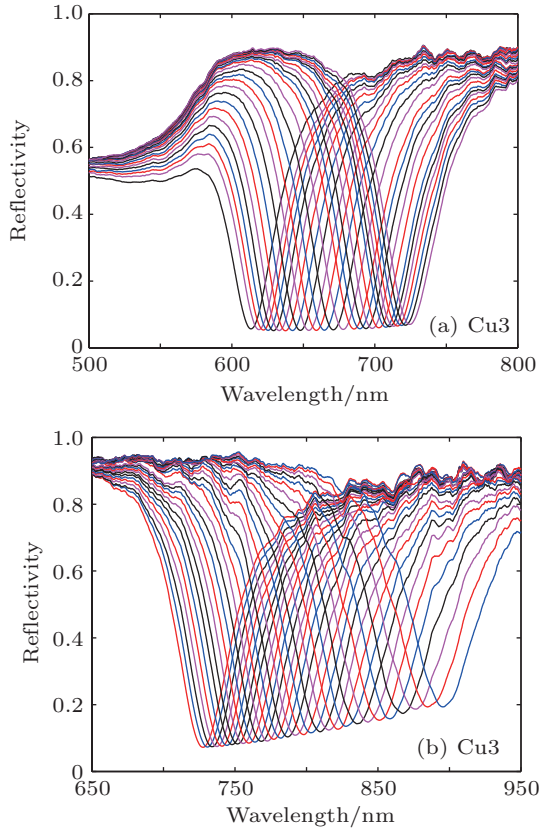


Fig. 5. (color online) Normalized SPR curves $R(\lambda)$ of Cu3 in the wavelength ranges: (a) from 613.50 nm to 724.59 nm, (b) from 727.45 nm to 895.36 nm.

The SPR curves $R(\theta)$ are shown in Fig. 6, in which not all curves are included for clear vision. We choose SPR curves $R(\theta)$ at several resonant wavelengths near 700 nm for comparison.

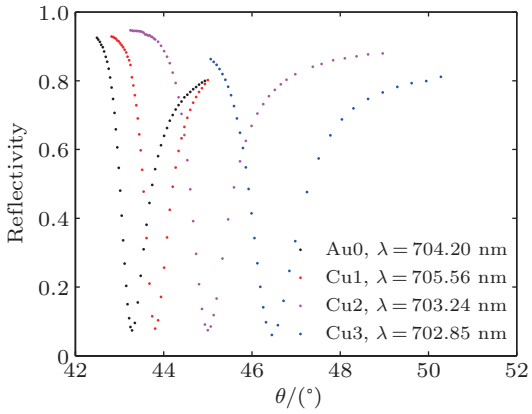


Fig. 6. (color online) Normalized SPR curves $R(\theta)$.

From all the SPR curves $R(\theta)$ obtained for the TiO_2-coated Cu films, it is concluded that the FWHM (full width at half maximum) of SPR curve $R(\theta)$ at a similar wavelength becomes larger as the thickness of TiO_2 increases, and for each TiO_2-coated Cu film, the FWHM decreases with increasing incident wavelength, which is consistent with the theoretical calculation.

To determine the effective optical constants of the films, the one-layer model is used because the consideration presented here is restricted to idealized films. The formulas of reflectivity R of p-polarization from the three-layer Kretchmann SPR configuration are employed. Take one film as an example, from each normalized SPR curve $R(\lambda)$, we can extract the resonant wavelength λ_{SPR}, the corresponding angle of incident θ_{SPR}, and the minimum reflectivity $R^{\mathrm{e}}_{\mathrm{min}}$. The $\varepsilon_{\mathrm{r}}(\lambda)$, $\varepsilon_{\mathrm{i}}(\lambda)$, and d are taken as adjustable parameters, and their possible ranges are set. Here $\varepsilon_{\mathrm{r}}(\lambda)$ and d are the real part of the effective optical constant and the effective thickness of the film, respectively. For a given d within the set range, two sets of $\varepsilon_{\mathrm{r}}(\lambda)$ and $\varepsilon_{\mathrm{i}}(\lambda)$ can be calculated for each λ_{SPR} using the criterion function $R^{\mathrm{t}}_{\mathrm{min}}[\varepsilon_{\mathrm{r}}(\lambda), \varepsilon_{\mathrm{i}}(\lambda)] - R^{\mathrm{e}}_{\mathrm{min}} = 0$, where $R^{\mathrm{t}}_{\mathrm{min}}$ represents the minimum reflectivity of the theoretical SPR curve. Then we can obtain two different sets of effective optical constants $\varepsilon(\lambda)$, each set consists of a set of $\varepsilon_{\mathrm{r}}(\lambda)$ and related $\varepsilon_{\mathrm{i}}(\lambda)$ for all λ_{SPR}. Assume x to be a set of the parameters $\varepsilon(\lambda)$ and d. As d is adjusted with a set step (1 nm), many sets of x are obtained. To determine the true solution of effective optical constants and thickness, a best fit is determined by computing the minimization of the objective function $F(x)$ defined as

$$F(x) = \left[\left(\sum_{i}^{N} \left[R^{\mathrm{t}}_{i}(x) - R^{\mathrm{e}}_{i} \right]^2 \right) / N \right]^{1/2}, \qquad (1)$$

where $R_i^{\mathrm{t}}(x)$ is the theoretical reflectivity, R_i^{e} is the experimental reflectivity, and i is a subscript for each of the N data points. In calculations, 200 data points near the SPR dip are sampled for each SPR curve $R(\lambda)$, so here $N = 200$. Among many sets of x, the unique solution which minimizes $F(x)$ can be simply selected.

Using the algorithm mentioned above, the effective optical constants of the films are determined, and the results are shown in Fig. 7. The effective thickness is 55 nm for Au0; 70 nm, 82 nm, and 94 nm for Cu1, Cu2, and Cu3, respectively. As depicted in Fig. 7, both $|\varepsilon_{\mathrm{r}}(\lambda)|$ and $\varepsilon_{\mathrm{i}}(\lambda)$ at a given wavelength decrease as the thickness of TiO_2 increases. In the case of Au0, the results agree closely with the ones from our previous work,[52] the discrepancy might arise from the difference of surface roughness between the films. The major contributions to the experimental errors arise from the absolute angle measurement errors, the light source instability, the optical resolution of the spectrometer, and the light beam divergence. The discussion about the experimental errors has been given previously,[52] the errors will not be estimated in this work because the errors could be smaller if a broadband source and a spectrometer with higher performance are employed.

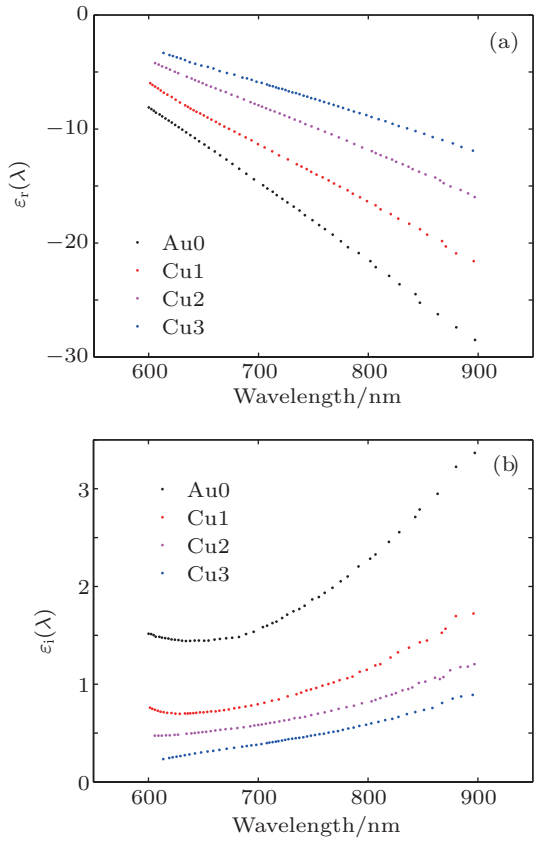


Fig. 7. (color online) Effective optical constants: (a) real part, (b) imaginary part.

To investigate the sensitivities of prism-based SPR sensors in which the films are employed, the ratio between the resonant angle or wavelength shift and the refractive index change is defined as the sensitivity versus angle or wavelength, expressed as S_θ or S_λ. Assuming that the refractive index of analyte changes from 1.33 to 1.34, we calculate S_θ and S_λ of the four films, and the results are shown in Fig. 8.

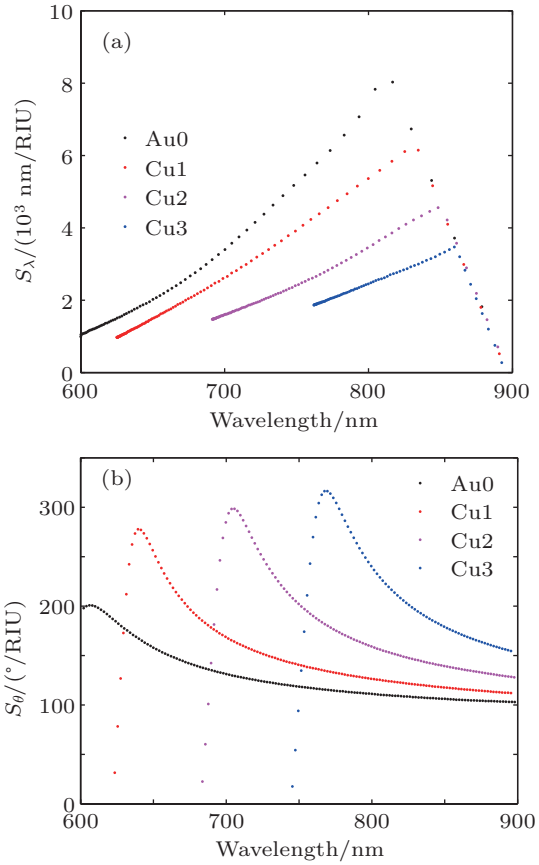


Fig. 8. (color online) (a) Sensitivity for wavelength modulation, (b) sensitivity for angular modulation, where RIU stands for refractive index unit.

As illustrated in Fig. 8, S_λ increases with increasing wavelength for each film until S_λ maximized, the maximum S_λ of Au0 is larger than that of Cu1, Cu2, and Cu3. For S_θ, there is an optimized wavelength which maximizes the S_θ for each film. For the TiO_2-coated Cu films, the optimized wavelength increases with increasing thickness of the TiO_2 film, and the maximum S_θ is larger than that of Au0. The phenomenon can be explained by the electromagnetic field distribution in our multilayer structure. It has been demonstrated that sensitivity enhancement mechanisms are accompanied with a field enhancement and correlated with the overlap integral in the analyte region. In brief, the sensitivity is governed by the ratio between the overlap integral in the analyte region and the total energy of the propagating mode, further more, the overlap integral combines the enhanced field amplitude in the analyte interface and the penetration depth into the analyte region.[54] The existence of the TiO_2 film, which enhances the field amplitude in the analyte interface, accounts for the sensitivity enhancement. However, the enhancement of

sensitivity does not scale linearly with the wavelength as one might expect from the increase of the interaction volume (integral volume), because the film becomes more absorptive in the infrared region. As a result, according to the effective optical properties of the films, there exist maximum sensitivities for both wavelength and angular modulations. Further calculations confirm that the maximum S_θ is also dependent on the refractive index of the dielectric medium, therefore, one can achieve a higher S_θ using the TiO_2-coated Cu film through optimizing the incident wavelength and the thickness of the TiO_2 film against the refractive index changes of analyte to be measured.

4. Conclusion

We present a new analytical method based on the surface plasmon resonance (SPR) technique, with which SPR curves for both wavelength and angular modulations can be obtained simultaneously via only a single scan of the incident angle. This method is particularly suitable for studying the plasmonic properties of SPR-compatible films due to its distinct advantage of convenience. Using this method, the SPR responses of an Au film and TiO_2-coated Cu films are characterized in the wavelength range from 600 nm to 900 nm at room temperature. For the first time, we determine the effective optical constants and the thicknesses of TiO_2-coated Cu films using the SPR curves of wavelength modulation. In addition, from the theoretical analysis of sensitivity, we can draw the conclusion that in the case of sensitivity with wavelength modulation, TiO_2-coated Cu films are not as good as the Au film, however, they are more suitable than the Au film for SPR refractive index sensors with angular modulation because a higher sensitivity can be achieved. Moreover, TiO_2-coated Cu films have the potential use for SPR sensors due to the low cost of Cu and good sensing properties of TiO_2.

References

[1] Rhodes C, Franzen S, Maria J P, Losego M, Leonard D N, Laughlin B, Duscher G and Weibel S 2006 *J. Appl. Phys.* **100** 054905
[2] Franzen S 2008 *J. Phys. Chem. C* **112** 6027
[3] Rhodes C, Cerruti M, Efremenko A, Losego M, Aspnes D E, Maria J P and Franzen S 2008 *J. Appl. Phys.* **103** 093108
[4] Franzen S, Rhodes C, Cerruti M, Gerber R W, Losego M, Maria J P and Aspnes D E 2009 *Opt. Lett.* **34** 2867
[5] Losego M D, Efremenko A Y, Rhodes C L, Cerruti M G, Franzen S and Maria J P 2009 *J. Appl. Phys.* **106** 024903
[6] Noginov M A, Gu L, Livenere J, Zhu G, Pradhan A K, Mundle R, Bahoura M, Barnakov Y A and Podolskiy V A 2011 *Appl. Phys. Lett.* **99** 021101
[7] Chen N C, Lien W C, Liu C R, Huang Y L, Lin Y R, Chou C, Chang S Y and Ho C W 2011 *J. Appl. Phys.* **109** 043104
[8] Soref R, Peale R E and Buchwald W 2008 *Opt. Express* **16** 6507
[9] Guske J T, Brown J, Welsh A and Franzen S 2012 *Opt. Express* **20** 23215
[10] Otto A and Sohler W 1975 *Solid State Commun.* **16** 1319
[11] Fontana E, Pantell R H and Moslehi M 1988 *Appl. Opt.* **27** 3334
[12] Tamm I R, Dawson P, Connolly M P, Raza S H and Gamble H S 1991 *J. Mod. Opt.* **38** 1593
[13] Mcneill D A, Morrow T and Dawson P 1998 *Appl. Surf. Sci.* **127–129** 46
[14] Cairns G F, Mcneill D A and Dawson P 1999 *Surf. Sci.* **429** 117
[15] Ma S M, Han B M, Jo J H and Chang S 2000 *J. Korean Phys. Soc.* **37** 788
[16] Mitsushio M, Watanabe K, Abe Y and Higo M 2006 *Sens. Actuators A* **125** 296
[17] Jha R and Sharma A K 2009 *Opt. Lett.* **34** 749
[18] Mitsushio M, Watanabe K, Abe Y and Higo M 2010 *Sens. Actuators A* **163** 1
[19] Diaz-Herrera N, Gonzalez-Cano A, Viegas D and Santos J L 2010 *Sens. Actuators B* **146** 195
[20] Schulz L G 1954 *J. Opt. Soc. Am.* **44** 358
[21] Roberts S 1960 *Phys. Rev.* **118** 1509
[22] Ehrenreich H and Phillip H R 1962 *Phys. Rev.* **128** 1622
[23] Stoll M Ph 1969 *J. Appl. Phys.* **40** 4533
[24] Johnson P B and Christy R W 1972 *Phys. Rev. B* **6** 4370
[25] Johnson P B and Christy R W 1974 *Phys. Rev. B* **11** 1315
[26] Hanekamp L J, Lisowski W and Bootsma G A 1982 *Surf. Sci.* **118** 1
[27] Doremus R, Shou C K and Garcia R 1992 *Appl. Opt.* **31** 5773
[28] Dobierzewska-Mozrzymas E and Bieganski P 1993 *Appl. Opt.* **32** 2345
[29] Urban III F K, Hosseini-Tehrani A, Khabari A, Griffiths P and Fernandez G 1999 *Thin Solid Films* **355–356** 513
[30] Stahrenberg K, Herrmann Th, Wilmers K, Esser N and Richter W 2001 *Phys. Rev. B* **64** 115111
[31] Du H, Lee S W, Gong J, Sun C and Wen L S 2004 *Mater. Lett.* **58** 1117
[32] Chan G H, Zhao J, Hicks E M, Schatz G C and Van Duyne R P 2007 *Nano Lett.* **7** 1947
[33] Zynio S A, Samoylov V, Surovtseva E R, Mirsky V M and Shirshov Y M 2002 *Sensors* **2** 62
[34] Ong B H, Yuan X, Tjin S C, Zhang J and Ng H M 2006 *Sens. Actuators B* **114** 1028
[35] Gupta B D and Sharma A K 2005 *Sens. Actuators B* **107** 40
[36] Chen X and Jiang K 2010 *Opt. Express* **18** 1105
[37] Lee A H, Roh S Y and Park J H 2009 *Opt. Fiber Technol.* **15** 209
[38] Manera M G, Leo G, Curri M L, Cozzoli P D, Rella R, Siciliano P, Agostiano A and Vasanelli L 2004 *Sens. Actuators B* **100** 75
[39] Manera M G, Cozzoli P D, Curri M L, Leo G, Rella R, Agostiano A and Vasanelli L 2005 *Synth. Met.* **148** 25
[40] Manera M G, Leo G, Curri M L, Comparelli R, Rella R, Agostiano A and Vasanelli L 2006 *Sens. Actuators B* **115** 365
[41] Manera M G, Cozzoli P D, Leo G, Curri M L, Agostiano A, Vasanelli L and Rella R 2007 *Sens. Actuators B* **126** 562
[42] Manera M G, Spadavecchia J, Buso D, Julian Fernandez C de, Mattei G, Martucci A, Mulvaney P, Perez-Juste J, Rella R, Vasanelli L and Mazzoldi P 2008 *Sens. Actuators B* **132** 107
[43] Manera M G, Taurino A, Catalano M, Rella R, Caricato A P, Buonsanti R, Cozzoli P D and Martino M 2012 *Sens. Actuators B* **161** 869
[44] Manera M G and Rella R 2013 *Sens. Actuators B* **179** 175
[45] Innes R A and Sambles J R 1987 *J. Phys. F: Met. Phys.* **17** 277
[46] Zhang S, Berguiga L, Elezgaray J, Roland T, Faivre-Moskalenko C and Argoul F 2007 *Surf. Sci.* **601** 5445
[47] Gu J H, Cao Z Q, Shen Q S and Chen G 2008 *J. Phys. D: Appl. Phys.* **41** 155309
[48] Lee W J, Kim J E, Park H Y, Park S, Kim M S, Kim J T and Ju J J 2008 *J. Appl. Phys.* **103** 073713
[49] Levesque L 2011 *Opt. Laser Technol.* **43** 14
[50] Velinov T, Ahtapodov L, Nelson A, Gateshki M and Bivolarska M 2011 *Thin Solid Films* **519** 2093
[51] Homola J, Yee S S and Gauglitz G 1999 *Sens. Actuators B* **54** 3
[52] Huang Y, Ye H A, Li S Q and Dou Y F 2013 *Chin. Phys. B* **22** 027301
[53] Zhang F and Zhong J G 2006 *J. Optoelectronics. Laser* **17** 211
[54] Shalabney A and Abdulhalim I 2010 *Sens. Actuators A* **159** 24